

# A Statistical Approach to Spectrum Measurement Processing

Dinesh Datla

Alexander M. Wyglinski

Gary J. Minden

Information and Telecommunication Technology Center  
The University of Kansas, Lawrence, KS 66045  
Email: {dineshd, alexw, gminden}@ittc.ku.edu

## Abstract

Prior knowledge of the spectrum behavior can greatly assist in efficiently performing dynamic spectrum access. This knowledge can be obtained by surveying the spectrum activity, which involves spectrum data collection, primary signal detection, and data analysis. One approach to signal detection is to perform energy detection based on the power measurements. Although considered optimal, this approach requires prior knowledge of the noise statistics in order to compute the signal threshold. In this paper, we present several algorithms for estimating the threshold directly from the spectrum measurement data. Both Otsu's and the recursive one-sided hypothesis testing (ROHT) algorithms, as well as the proposed recursive Otsu's algorithm, have been applied to spectrum measurements collected from an FM broadcast band and a digital television band. The results show that the proposed algorithm performed well, with nearly 100% detection probability, when applied on the DTV band measurements. However, it was not able to provide the same performance for the FM band measurements.

## 1 Introduction

Dynamic spectrum access (DSA) networks can optimize the spectrum utilization, thereby avoiding the potential for spectrum scarcity. Although DSA networks offer numerous benefits, their actual implementation faces several challenges [1]. In a DSA network, one important challenge is the simultaneous coexistence of an unlicensed user (i.e., the secondary user) with a licensed user (i.e., the primary user) while not interfering with each other. This requires that the unlicensed user possesses thorough knowledge of its spectrum operating conditions, including the dynamics of the spectrum occupancy, as well as the characteristics of the primary signals occupying the spectrum. For instance, using *a priori* knowledge of the spectrum utilization statistics, the secondary user is capable of making predictions on the future availabil-

ity of the spectrum and accordingly initiate secondary transmissions [2]. This knowledge about the spectrum occupancy can be gained via *spectrum surveying*.

Spectrum surveying involves the long term collection of spectrum data, data processing for detecting signal presence, and data analysis for characterizing the spectrum occupancy [3]. Primary signal detection is vitally important in any spectrum survey. Among the different signal detection techniques presented in the literature [4], energy detection is the optimal method for the detection of signals based on power measurements [5]. In energy detection, a measurement sample is classified either as a signal if the measured power exceeds a decision threshold or as noise otherwise.

While there are several existing methods to estimate the decision threshold [2, 6–9], they possess several drawbacks, such as the need for *a priori* knowledge about the noise statistics or the properties of the primary user transmissions. This paper presents and compares the *recursive one-sided hypothesis testing* (ROHT) [3, 10], Otsu's algorithm [11], and the proposed recursive Otsu's algorithms. These algorithms have the ability to estimate the decision threshold from the measurement data without requiring any *a priori* knowledge. While the ROHT and Otsu's algorithms have been previously proposed, the recursive Otsu's algorithm is proposed in this paper and compared with the other two algorithms.

The rest of the paper is organized as follows: Section 2 provides an overview of the past methods for threshold estimation, including Otsu's algorithm. The ROHT and the recursive Otsu's algorithms are presented in Section 3. The results of applying the ROHT, Otsu's, and the proposed recursive Otsu's algorithms on actual spectrum measurements are presented in Section 4. We end this paper with several concluding remarks in Section 5.

## 2 Previous Threshold Estimation Methods

An important step in energy detection is the estimation of the decision threshold. The decision threshold can be estimated using several techniques, such as:

---

This work was supported by NSF grants ANI-0230786 and ANI-0335272.

1. Empirical data analysis,
2. Computation of threshold as a function of receiver properties,
3. Using *a priori* knowledge of noise statistics and spectrum occupancy, and
4. Analysis of measurement data histogram.

The simplest approach for determining the threshold is via an empirical analysis wherein the collected measurements can be visually inspected before setting an appropriate threshold [6, 7]. In the second approach, the decision threshold can be computed as a function of the sensitivity and noise figure of the receiver [6, 8]. The threshold can also be determined from the cumulative density function (CDF) that is computed from the measurement data as discussed next.

## 2.1 Threshold Estimation Based on Cumulative Density Function Analysis

By measuring a vacant channel that is free from external interference, samples of both the system and ambient noise can be collected and used for computing an inverse CDF. If  $S$  is a random variable representing the measured noise power, the inverse CDF (ICDF) of  $S$  can be defined as  $ICDF(S, X) = P(S \geq X)$ . If  $X$  is the decision threshold, then the corresponding false alarm probability will be  $ICDF(S, X)$ . From the ICDF, the threshold can be chosen for a fixed false alarm probability [2, 9].

Suppose we collect power measurements<sup>1</sup> from a target band in the spectrum, a matrix of spectrum measurements can be represented by  $\mathbf{M}$ , where  $H$  denotes a random variable representing the measured power. The CDF of  $H$  computed from  $\mathbf{M}$  can be defined as:

$$CDF(H, \mathbf{M}) = P(H \leq M(f_i, t_j)), M(f_i, t_j) \in \mathbf{M}, \quad (1)$$

where  $M(f_i, t_j)$  represents a sample of the power measured at frequency  $f_i$  and time instance  $t_j$ . Based on this CDF, simple techniques can be used to classify the spectrum measurements. The next two examples will illustrate this approach.

**Example 1:** The threshold is chosen based on *a priori* knowledge about the spectrum utilization via a process known as  $p$ -tile thresholding [12]. For instance, if it is known that the fraction of the spectrum being utilized is  $p$ , then choose a threshold  $T$  such that  $p$  fraction of the measurements have values

greater than  $T$ , i.e.

$$1 - p = CDF(H = T, \mathbf{M}). \quad (2)$$

Fig. 1 shows the CDF computed from the FM band (88-108 MHz) measurements. The figure illustrates the process of  $p$ -tile thresholding where the threshold is estimated to be  $T = -87.2 \text{ dBm}$  for  $p = 0.5$ .

**Example 2:** Compute a marginal CDF, denoted by  $CDF_{f_i}$ , for each frequency in the sweep bandwidth and classify a frequency channel  $f_i$  based on the statistic of  $CDF_{f_i}$ . For instance, determine the maximum measurement for frequency channel  $f_i$  and if the maximum is above a certain threshold, classify  $f_i$  as an occupied frequency channel. This threshold can be manually set based on some factors, such as the noise floor of the measurement subsystem.

The threshold based classification of the spectrum measurements can also be performed by analyzing the histogram of the measurement data.

## 2.2 Threshold Estimation Based on Histogram Analysis: Mode Method

The global histogram of the spectrum measurements can be bimodal<sup>2</sup>. In a bimodal histogram, the two peaks belong to the signal and noise samples, respectively. When measurements are collected and organized with respect to frequency, the values of the measurements collected from the edges<sup>3</sup> of the channels occupied by the signals occur less frequently in the measurement data as compared to the signal and noise measurements. Thus, the valley between these peaks in a measurement data histogram may belong to the measurement values at the edges of the signals. Thus, the value of the local minimum between the two peaks, or the center point (mean) between the peaks, can be chosen as the decision threshold [12] (see Fig. 2). When the mode method was applied on FM band (88-108 MHz) measurements, a miss rate of 17.32% and a false alarm rate<sup>4</sup> of 23.62% was observed.

If we consider a sparsely occupied band, such as the upper TV band (54-87 MHz) where a large portion of the band is vacant and occupied by background noise, the histogram may not be bimodal as seen from Fig. 3. In such cases, additional processing has to be done to make the histogram bimodal [12]. The Laplacian operator is applied to  $\mathbf{M}$ . The Laplacian forms the spatial second partial derivative of a function  $F(x, y)$

<sup>2</sup>A bimodal histogram consists two peaks.

<sup>3</sup>Boundary separating the band of frequencies occupied by a signal from the adjacent vacant channels occupied by noise.

<sup>4</sup>The miss rate and the false alarm rate have been defined in reference [3].

<sup>1</sup>In this case the power measurements capture both the signal as well as the noise presence in the frequency band being measured.

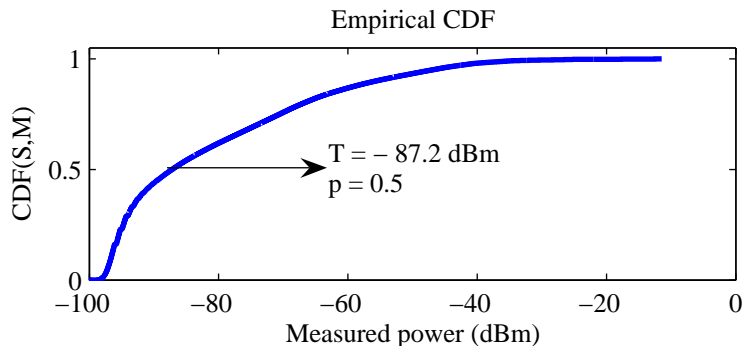


**Fig. 1** CDF plot of the FM band measurement data. Threshold  $T$  for  $p = 0.5$  is determined from CDF.

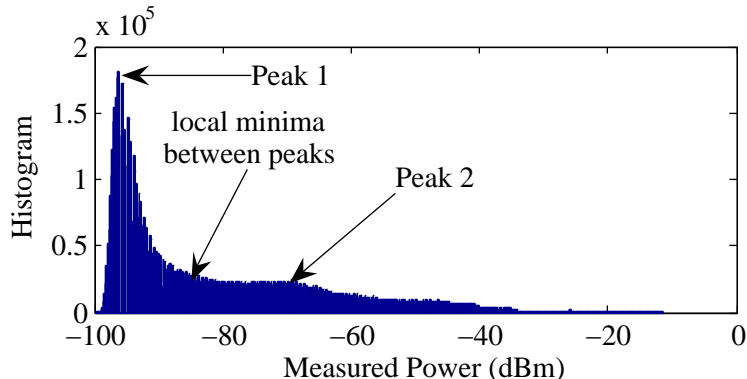


**Fig. 2** Histogram of the FM band (88-108 MHz) measurements.

(i.e., the rate of change in slope) and has the mathematical form [12]:

$$G(x, y) = -\nabla^2 \{ F(x, y) \} \quad (3)$$

where  $\nabla^2 = \frac{\partial^2}{\partial x^2} + \frac{\partial^2}{\partial y^2}$ .

Consider the case when a signal is surrounded by uniform noise<sup>5</sup> present in the adjacent channels. Ideally, at the signal edges the measurement values increase from a low plateau level (belonging to the uniform background noise) to the peak power level of the signal waveform in a smooth ramp-like manner. In the plateau and along the ramp where the slope is constant, the Laplacian is zero. However, in the regions where there is a transition from the low plateau to the ramp or from the ramp to the signal peak, the Laplacian has a large magnitude. A histogram formed only from measurement samples located at coordinates corresponding to a high magnitude of Laplacian is expected to be bimodal [12].

The *laplacian threshold*  $L(n) = \mu_L + (n \sigma_L)$  is used to identify the high magnitude Laplacian values, where  $\mu_L$  and  $\sigma_L$  are the mean and standard deviation of the Laplacian values, and  $n$  is a positive

integer which can be specified. Fig. 3 shows the normalized histogram of the TV band (54-87 MHz) measurements with Laplacian greater than  $L(4)$ . Fig. 4 shows the results for the classification of TV band (54-87 MHz) data for different values of  $L(n)$ . As seen from Fig. 4, the best classification has been obtained for  $n = 4$ .

In all these methods, the noise variance is reduced by averaging the data. Furthermore, the threshold can be set lower for the same false alarm rate, resulting in an increase in the probability of detection of weak signals.

The drawbacks of these threshold estimation techniques are: (i) the threshold estimated is specific to the receiver, and hence fails to detect the presence of signals that occur below the receiver's noise floor, (ii) these methods require *a priori* knowledge of the noise statistics or the spectrum occupancy, and (iii) the classification is dependent upon manually selecting a threshold value. For instance, the local minima in the mode method has to be selected manually. This approach can be automated by analytically representing the shape of the histogram and then performing an optimization of this analytical expression. However, such methods are not always accurate [12]. Due to these drawbacks, these classification techniques cannot be implemented in an automated fashion in a cog-

<sup>5</sup>Noise that does not vary significantly across the target frequency band.

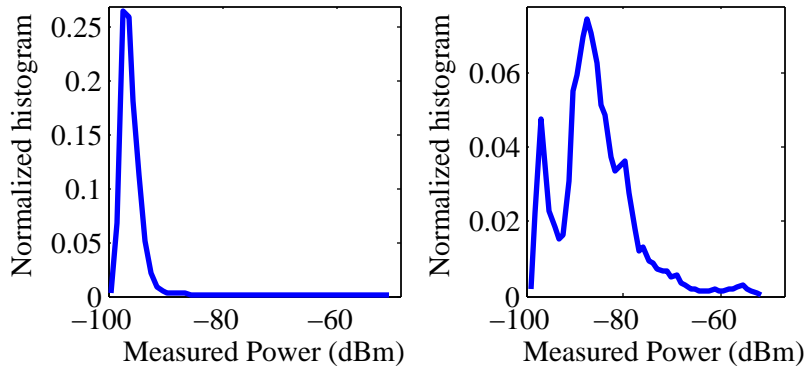


**Fig. 3** Normalized histogram of the Upper TV band (54-87 MHz) measurement data (left), and normalized histogram of selected samples in the TV band data (right).

nitive radio.

While the above methods require *a priori* knowledge, we present in this paper three algorithms that estimate the threshold directly from the data itself without requiring any *a priori* knowledge. One of the three algorithms which has been presented in Reference [11] is discussed next.

### 2.3 Optimum Thresholding using Otsu's Algorithm

Otsu's algorithm selects an optimum threshold based on the properties of the histogram of the data and it does not assume any model for the histogram [11]. The optimum threshold yields maximum separation between the two classes of data, namely the signal and noise classes. The algorithm also returns a metric that indicates the separability of the two classes, which is useful to quantify the *goodness* of the threshold. Before applying Otsu's algorithm, the measurement data in  $\mathbf{M}$  is converted to a gray scale image  $\mathbf{I}$ .

The data is quantized into  $L$  levels with values  $s \times [1, 2, \dots, L]$ , where  $s$  is a scaling factor. Let the  $i^{\text{th}}$  gray level value be denoted by  $g_i$  and its probability of occurrence be denoted by  $p_i$ . The mean of the distribution is defined as:

$$\mu_T = \sum_{i=1}^L g_i \cdot p_i.$$

A threshold,  $T = g_k$ , can be used to bifurcate the probability distribution into the noise class  $C_0$  and the signal class  $C_1$ , with the levels  $[1, 2, \dots, k] \in C_0$  and levels  $[k + 1, \dots, L] \in C_1$ . For a certain threshold set at the  $k^{\text{th}}$  gray level, the *between-class variance* is defined as [11]:

$$\sigma_B^2(k) = \frac{[\mu_T \omega_k - \mu(k)]^2}{\omega_k(1 - \omega_k)} \quad (4)$$

$$\text{where } \omega_k = \sum_{i=1}^k p_i, \quad (5)$$

$$\text{and } \mu(k) = \sum_{i=1}^k g_i p_i. \quad (6)$$

A measure of class separability can be defined as [11]:

$$\alpha = \sigma_B^2 / \sigma_T^2. \quad (7)$$

Otsu's algorithm is an optimization problem that involves determining the gray level of the optimum threshold,  $k^*$ , that maximizes the above defined measure of class separability:

$$\alpha(k^*) = \max_{1 \leq k < L} \sigma_B^2(k) / \sigma_T^2. \quad (8)$$

A simple way of determining the optimum threshold would be by varying the threshold in steps computing the measure of separability and then choosing the threshold that gives the maximum value for this measure.

The next section describes the proposed recursive Otsu's algorithm as well as the previously published ROHT algorithm [3, 10].

### 3 Recursive Thresholding Classification Algorithms

In primary signal detection, one of the challenges is to detect signals with a high dynamic range. In the presence of strong signals, the threshold that is estimated from the spectrum data may not be low enough to identify the presence of weak signals. However, this challenge can be overcome by performing classification of the measurement data in a recursive manner.

Before performing classification of spectrum measurements, some pre-processing is performed on the data in order to condition the data and make it suitable for classification [3]. The histogram of the measurement data is clipped at both the left as well as right ends of the histogram at power levels  $nc$  and  $sc$ .



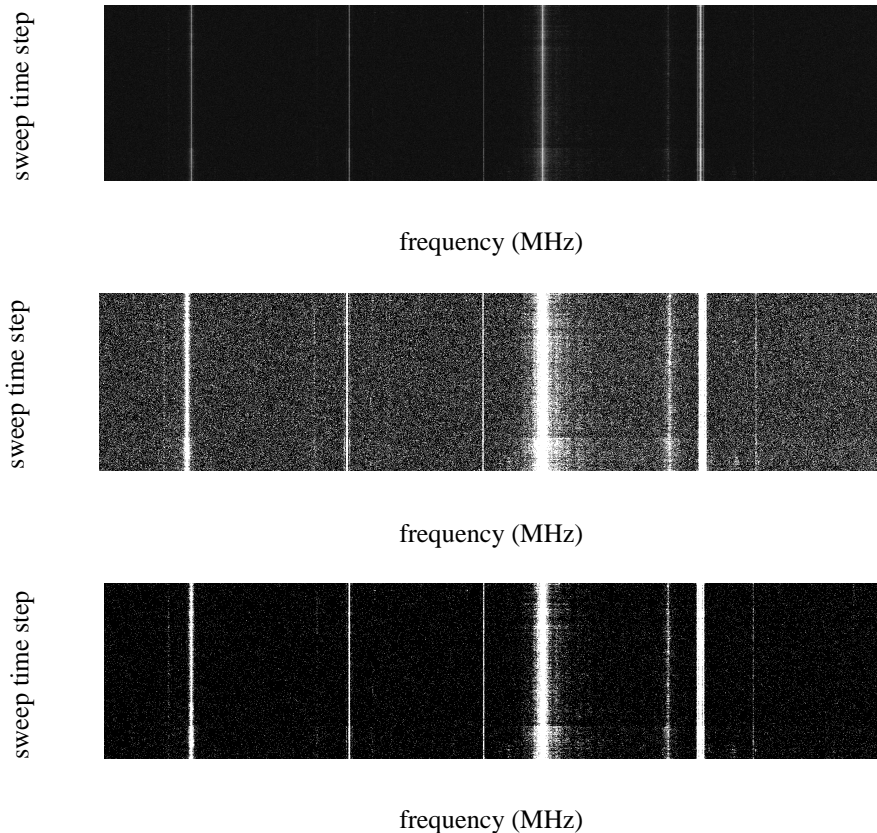


**Fig. 4** Classification results of TV band (54-87 MHz) measurements using various values of  $L(n)$  (from top to bottom):(a) original spectrum image, (b) image of data classified with  $n = 2$ , (c) image of data classified with  $n = 4$ .

A spatial averaging filter and a Gaussian low pass filter, each of length  $L$ , can be used in cascade in order to perform noise filtering. Thus, the parameters of the data enhancement operations are specified by  $L$ ,  $sc$ , and  $nc$ . Furthermore, the measurement samples can be time averaged in order to reduce the variance of noise.

The recursive one-sided hypothesis testing (ROHT) algorithm [3, 10] performs classification of the spectrum measurements based on the concept of one-sided hypothesis testing. The algorithm works for various levels of statistical significance. One drawback with the ROHT algorithm is that not all distributions are Gaussian. In addition, central limit theorem is applicable only when there are a large number of samples available such that the actual distribution converges to the Gaussian distribution.

The proposed recursive Otsu's algorithm has been adapted from the original recursive method presented in Reference [13]. The proposed algorithm has been modified such that it functions similar to that of the ROHT algorithm.

With these recursive algorithms, the measurement data is initially assumed to contain mostly noise samples. Fig. 5 shows the flowchart of the recursive

thresholding. By applying one-sided hypothesis test or Otsu's algorithm the threshold is estimated. This threshold is employed to identify a percentage of the measurement data as signal samples and the rest as noise. The signal portion is discarded and this process is repeated iteratively on the remaining unclassified measurements until the change in the standard deviation of the unclassified data between two consecutive iterations becomes less than or equal to  $\epsilon$ , where  $\epsilon$  is an arbitrary positive value that can be specified. The recursive Otsu's algorithms differ from the ROHT algorithm in that at every iteration the threshold is now estimated using Otsu's algorithm instead of the one-sided hypothesis testing employed in the ROHT algorithm.

In the case of the proposed recursive Otsu's algorithm, the argument that is passed to the algorithm is the  $\epsilon$  value. In these algorithms, the following notations have been used:

- $\mathbf{M}$  be the set of measurement samples,
- $S$  be the set of signals within  $\mathbf{M}$ ,
- $S_k$  be a subset of  $S$  for the  $k^{th}$  iteration of the algorithm,
- $Q$  be the set of noise samples within  $\mathbf{M}$ ,

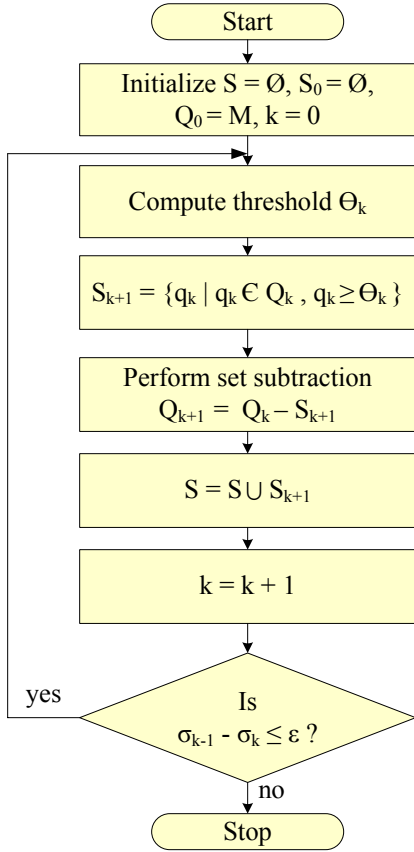


Fig. 5 Flowchart for recursive thresholding.

- $Q_k$  be a superset of  $Q$  for the  $k^{th}$  iteration of the algorithm,  $Q_k$  may contain signals,
- $\mu_k$ ,  $\sigma_k$  = mean and standard deviation of the elements of  $Q_k$ , and
- $\theta_k$  = decision threshold to identify the signal portion for the  $k^{th}$  iteration.

#### 4 Performance Evaluation of Processing Techniques

The spectrum measurement data employed in this work was collected in a rural environment at the Information and Telecommunications Technology Center at the University of Kansas, Lawrence, Kansas, USA, over a 24 hour period. Two spectrum bands have been targeted: the FM broadcast band (88-108 MHz) and the digital television band (DTV) (638-668 MHz). These bands have been chosen since licensing information is available for these bands whereas the television band is gaining popularity as the prime candidate for DSA.

##### 4.1 FM Broadcast Spectrum: 88-108 MHz

All the data enhancement operations were performed on the FM spectrum measurements in a cascade manner, followed by classification using the original Otsu's

algorithm. Table 1 presents the results for various values of the data enhancement parameters. In this table, the parameters are listed in the order of their occurrence in the cascade of operations.

From Table 1, it is evident that the data enhancement operations have improved the performance of original Otsu's classification algorithm. Case 2 shows improvement in the results as compared to Case 1, where the classification has been done without any data enhancement. Case 3 is worth noting for the improvement in the miss rate although the false alarm rate is degraded by a small percentage as compared to Case 2. Fig. 6 shows a single time sweep of the FM band measurement data after data enhancement (Case 3). In certain bands with fixed channelization, such as the FM and TV broadcast bands, most active licensees transmit continuously for 24 hours. In such cases, all the measurement sweeps of data collected across a band represent redundant data. By averaging over such redundant sweeps of data, which is affected by independent random noise, the noise variance is reduced, as shown in Fig. 7. The measurements were time averaged before applying the original Otsu's algorithm and the results are shown as Cases 5-7. It is observed that time averaging improves the false alarm rate since the noise power is reduced. Overall, the best results have been obtained by applying the data enhancement techniques along with the time averaging technique before the original Otsu's classification.

The ROHT algorithm was applied on the FM band data. The results of the ROHT algorithm with  $\epsilon = 0.5$  for various values of the confidence intervals are illustrated in Fig. 8, and also tabulated in Table 2(a). From the results, the tradeoff between miss rate and false alarm rate is clearly pronounced. As the confidence interval is increased from 90% to 99.9%, it is observed that the miss rate increases while the false alarm rate decreases. From the plots we can also infer that good results can be obtained for the FM band by operating the algorithm at around 96% confidence level beyond which the miss rate drastically increases. A similar trend has been observed for the case when  $\epsilon = 0.05$  as shown in Table 2(b). Table 2(c) shows the results of applying the modified recursive Otsu's algorithm on FM measurement data. The processed data can be used to study various aspects of spectrum occupancy such as the duty cycle as shown in Fig. 9.

##### 4.2 Digital Television Band: 638-668 MHz

A single time snapshot (instantaneous power spectrum) of the digital TV band (638-668 MHz) is shown in Fig. 10(a). In this figure, channel 44 can be observed at 650-656 MHz. It is also observed that there is substantial noise power variation in the instanta-

**Table 1** Results of applying data enhancement operations followed by the original Otsu’s algorithm on FM broadcast spectrum (88-108 MHz) measurement data.

Case No.	Parameters	Miss (%)	FA (%)	Error (%)	Weighted error (%)
1	No enhancement	24.9279	16.5625	18.8212	7.5345
2	$L = 4$	21.7692	14.4307	16.4121	6.5762
3	$sc = -55$ dBm, $nc = -98$ dBm, $L = 4$	17.4581	18.0527	17.8921	5.9834
4	$sc = -64$ dBm, $nc = -98$ dBm, $L = 4$	13.8231	21.9614	19.7641	5.5772
5	Time averaging and classification	22.7778	11.7123	14.7000	6.5100
6	$sc = -55$ dBm, $nc = -98$ dBm, $L = 4$ , time averaging	17.4074	15.4795	16.0000	5.6900
7	Time averaging, $sc = -55$ dBm, $nc = -98$ dBm, $L = 4$	18.1481	14.6575	15.6000	5.7700

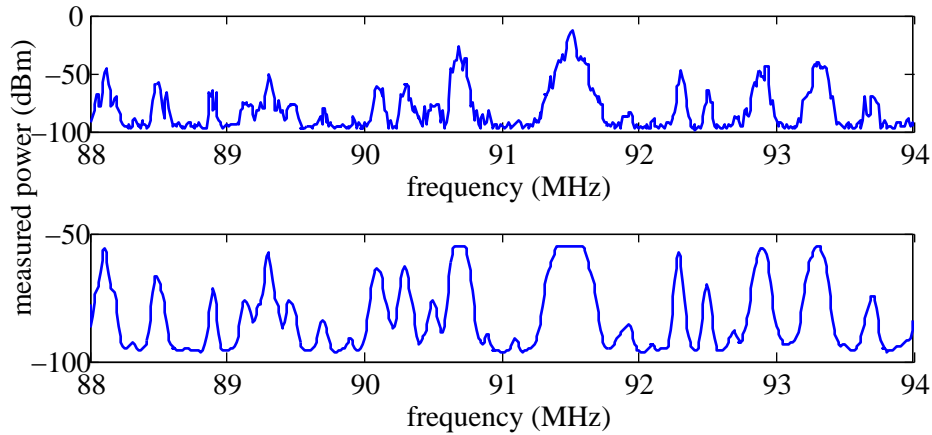


**Fig. 6** Power spectrum of FM band (88-94 MHz) before (top) and after data enhancement (bottom).

neous power spectrum, which can degrade the accuracy of classification algorithms. A comparison of Fig. 10(a) and Fig. 10(b) clearly shows that there is significant reduction in the noise variations by time averaging the data over 25 time snapshots. The time averaged data was then classified using the original Otsu’s algorithm.

Fig. 10(c) shows the result of applying ROHT (95% confidence level and  $\epsilon = 1.5$ ) algorithm on time averaged data. Similar classification result has been obtained by using the proposed recursive Otsu’s algorithm on the mean power spectrum.

When applied on the measurements collected from the analog television band (198-228 MHz), it was observed that the recursive Otsu’s algorithm gave a very high false alarm rate while both the ROHT as well as the original Otsu’s algorithm gave good results.

Overall, it has been observed that the original

Otsu’s algorithm performed well on all the three bands. The ROHT algorithm gave good performance with the television bands while the proposed recursive Otsu’s algorithm gave good performance only with the DTV band measurements. The reason for the high false alarm rate that is achieved while using the recursive Otsu’s algorithm is the small range of the signal power in the analog television band which results in noise being wrongly classified as signal. This implies that the recursive algorithms are well suited for detecting signals with a wide range of power levels.

## 5 Conclusions

In this paper, we present statistical techniques for the processing of spectrum measurements including the recursive one-sided hypothesis testing (ROHT) algorithm, Otsu’s algorithm, as well as the proposed recursive Otsu’s algorithm. In addition, we conducted

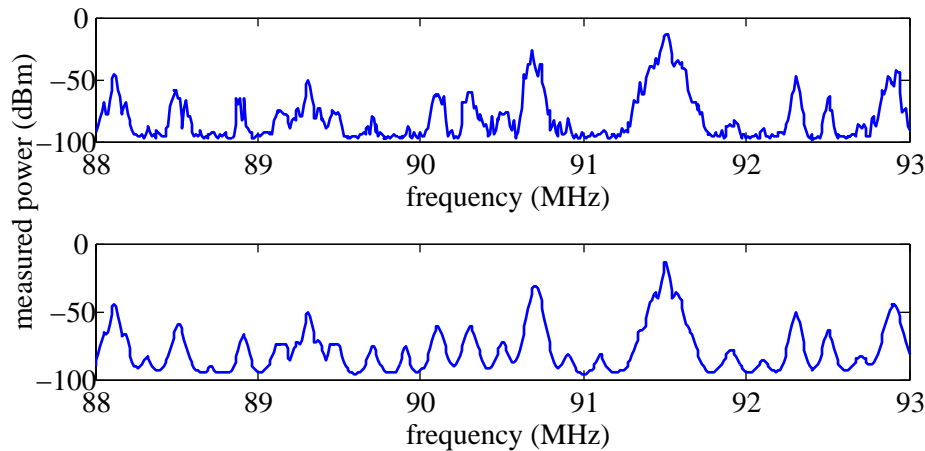


**Fig. 7** Power spectrum of the 88-93 MHz band in the FM broadcast spectrum before time averaging (top) and after time averaging (bottom).

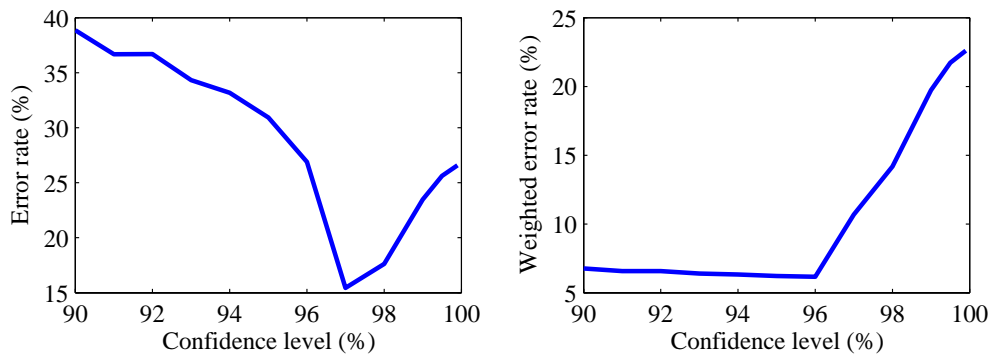


**Fig. 8** Results of ROHT algorithm with  $\epsilon = 0.5$  applied on FM band data (without data enhancement) for various confidence levels: error rate (left), and weighted error rate (right).

a comparison of the three algorithms and studied their performance on spectrum measurements collected from the FM band (88-108 MHz) and the digital television band (638-668 MHz). In addition, we have demonstrated improvement in the performance of the processing algorithms by conducting pre-processing operations on the spectrum measurements such as time averaging, and noise filtering.

The algorithms presented in this paper were able to estimate the threshold directly from the data itself without requiring any *a priori* knowledge and with minimum manual intervention in the threshold estimation.

## References

- [1] R. Rajbanshi, V. R. Petty, D. Datla, F. Weidling, D. DePardo, P. Kolodzy, M. J. Marcus, A. M. Wyglinski, J. B. Evans, G. J. Minden, and J. A. Roberts, "Feasibility of Dynamic Spectrum Access in Underutilized Television Bands," in *To appear in Second IEEE International Symposium on New Frontiers in Dynamic Spectrum Access Networks*, (Dublin, Ireland), April 2007.
- [2] S. D. Jones, N. Merheb, and I.-J. Wang, "An Experiment for Sensing-Based Opportunistic Spectrum Access in CSMA/CA Networks," in *IEEE International Symposium on New Frontiers in Dynamic Spectrum Access Networks*, (Baltimore, MD, USA), pp. 593–596, November 2005.
- [3] D. Datla, A. M. Wyglinski, and G. J. Minden, "A Framework for Spectrum Surveying in Dynamic Spectrum Access Networks," *Submitted to IEEE Journal on Selected Areas in Communications: Cognitive Radio: Theory and Applications*, 2007.
- [4] D. Cabric, S. M. Mishra, and R. W. Brodersen, "Implementation Issues in Spectrum Sensing for Cognitive Radios," in *Conference Record of the Thirty-Eighth Asilomar Conference on Signals, Systems and Computers*, vol. 1, (Pacific Grove, CA, USA), pp. 772–776, November 2004.
- [5] R. Tandra and A. Sahai, "Fundamental Limits on Detection in Low SNR Under Noise Uncertainty," in *International Conference on Wireless Networks, Communications and Mobile Computing*, vol. 1, pp. 464–469, 2005.
- [6] A. J. Petrin, *Maximizing the Utility of Radio Spectrum: Broadband Spectrum Measurements and Occupancy Model for Use by Cognitive Radio*. PhD thesis, School of Electrical and Computer Engineering, Georgia Institute of Technology, Atlanta, Georgia, USA, August 2005.
- [7] M. A. McHenry, "NSF Spectrum Occupancy Measurements Project Summary," tech. rep., Shared Spectrum Company, August 2005.
- [8] S. Ellingson, "Spectral Occupancy at VHF: Implications for Frequency-Agile Cognitive Radios," in *IEEE Vehic-*



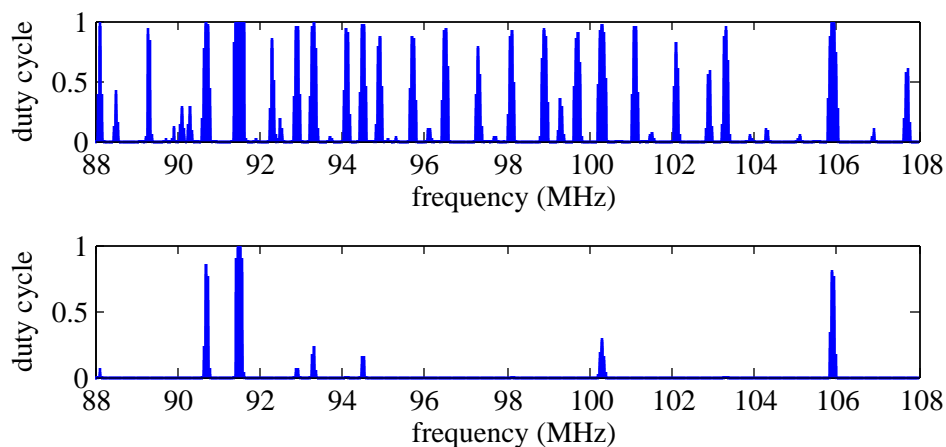


**Fig. 9** Results of ROHT algorithm with  $\epsilon = 0.5$  applied on FM band data (without data enhancement): Duty cycle plots for the confidence intervals of 98 % (top) and 99.5 % (bottom).

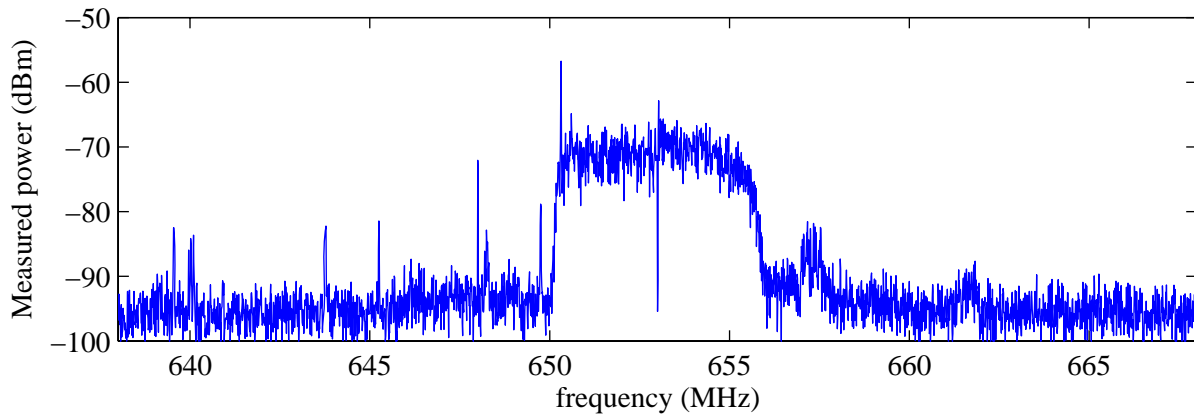
**Table 2** Performance evaluation of recursive thresholding applied to FM band (88-108 MHz) data: (a) ROHT algorithm with  $\epsilon = 0.5$ , (b) ROHT algorithm with  $\epsilon = 0.05$ , and (c) Recursive Otsu’s algorithm. Data enhancement with  $sc = -55$  dBm,  $nc = -98$  dBm, and  $L = 4$  has been performed to the data before thresholding.

[12] W. K. Pratt, *Digital Image Processing*. John Wiley & Sons, 3 ed.  
 [13] M. Cheriet, J. N. Said, and C. Y. Suen, “A Recursive Thresholding Technique for Image Segmentation,” *IEEE Transactions on Image Processing*, vol. 7, pp. 918–921, June 1998.

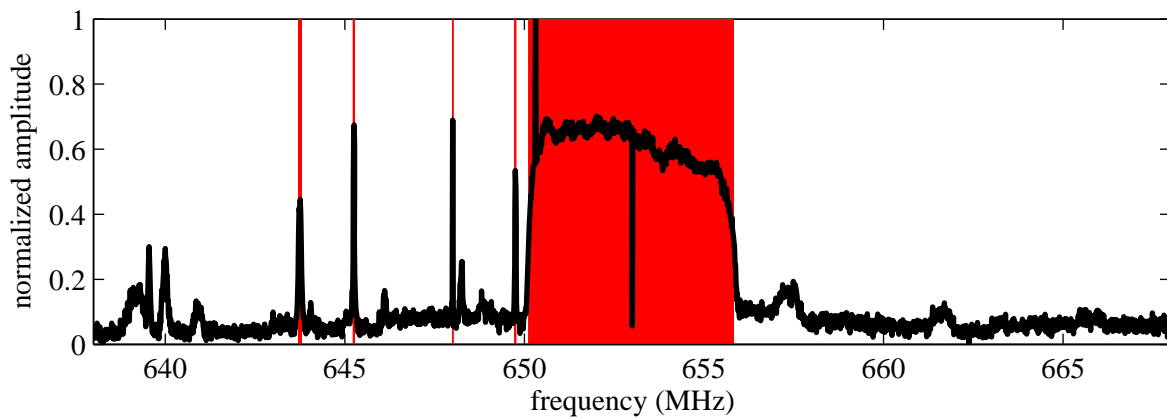
Confidence Level (%) / $\epsilon$	Miss (%)	FA (%)
(a) $\epsilon = 0.5$		
90	1.6985	50.5119
94	5.9117	34.5668
95	8.3757	29.6694
99.9	99.9702	0.0909
(b) $\epsilon = 0.05$		
90	0.0993	74.6542
92	0.1535	71.8168
95	0.5766	61.4434
99.9	99.9702	0.0909
(c) Rec. Otsu		
$\epsilon = 0.5$	0.0348	80.9202
$\epsilon = 1.5$	0.4211	64.1711

ular Technology Conference, vol. 2, (Dallas, TX, USA), pp. 1379–82, September 2005.

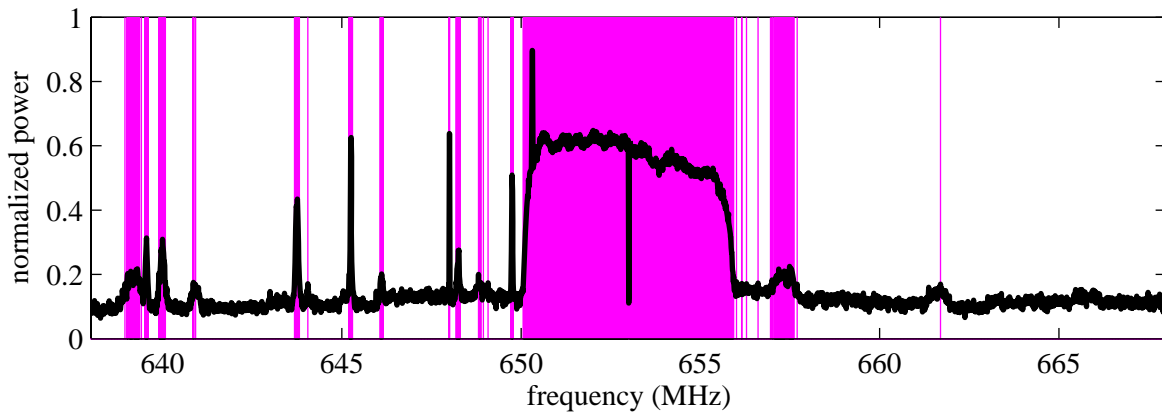
[9] J. R. Hoffman and R. J. Matheson, “RSMS Measurement and Analysis of LMR Channel Usage,” in *International Symposium on Advanced Radio Technologies*, (Boulder, CO, USA), pp. 13–19, March 2005.  
 [10] F. Weidling, D. Datla, V. Petty, P. Krishnan, and G. J. Minden, “A Framework for RF Spectrum Measurements and Analysis,” in *IEEE International Symposium on New Frontiers in Dynamic Spectrum Access Networks*, (Baltimore, MD, USA), pp. 573–576, November 2005.  
 [11] N. Otsu, “A Threshold Selection Method from Gray-Level Histograms,” *IEEE Transactions on Systems, Man, and Cybernetics*, vol. SMC - 9, pp. 62–66, January 1979.



(a) Instantaneous power spectrum of digital TV band (638-668 MHz).



(b) Digital TV band (638-668 MHz): original Otsu's classification (red) of averaged measurements (black).



(c) Digital television band (638-668 MHz): mean power spectrum (black) and its ROHT (95% confidence level and  $\epsilon = 1.5$ ) classification (magenta).

**Fig. 10** DTV measurements.